Encoding of Periodic and their Transient Motions by a Single Dynamic Movement Primitive

Johannes Ernesti*, Ludovic Righetti†‡, Martin Do*, Tamim Asfour*, Stefan Schaal†‡
*Institute for Anthropomatics, Karlsruhe Institute of Technology, Germany
†Computational Learning and Motor Control Lab, University of Southern California, Los Angeles, California
‡Department of Autonomous Motion, Max-Planck Institute for Intelligent Systems, Tübingen, Germany

***Abstract*—Present formulations of periodic dynamic movement primitives (DMPs) do not encode the transient behavior required to start the rhythmic motion, although these transient movements are an important part of the rhythmic movements (i.e. when walking, there is always a first step that is very different from the subsequent ones). An ad-hoc procedure is then necessary to get the robot into the periodic motion. In this contribution we present a novel representation for rhythmic Dynamic Movement Primitives (DMPs) that encodes both the rhythmic motion and its transient behaviors. As with previously proposed DMPs, we use a dynamical system approach where an asymptotically stable limit cycle represents the periodic pattern. Transients are then represented as trajectories converging towards the limit cycle, different trajectories representing varying transients from different initial conditions. Our approach thus constitutes a generalization of previously proposed rhythmic DMPs. Experiments conducted on the humanoid robot ARMAR-III demonstrate the applicability of the approach for movement generation.**

I. Introduction

The use of motion primitives to encode complex movements for robots and especially for humanoid robots has attracted a lot of attention the past years. The seminal work of Ijspeert et al. [1], [2] introduced the idea of Dynamic Movement Primitives (DMPs) which are primitives of motion that are encoded as a stable dynamical system. Both discrete (e.g. reaching) and rhythmic (e.g. walking) motions can be encoded with DMPs using two different canonical systems. Multi-dimensional coordinated behaviors can be easily generated and the modulation of simple order parameters allows to generalize the motion to different places in the workspace with smooth transitions in frequencies and amplitudes. DMPs have been successfully used as compact representations for imitation learning [1], [2] or reinforcement learning [3] and their representation as stable dynamic systems allows online trajectory generation for obstacle avoidance [4] or sensory feedback inclusion to improve manipulation performance [5].

While a lot of attention has been given to discrete DMPs, the literature on rhythmic DMPs is more scarce [2], [6], [7], [8]. Meanwhile, a lot of attention has also been given on Central Pattern Generators (CPGs) in locomotion control. This concept comes from animal locomotion, where CPGs are neural networks located in the spinal cord of vertebrates that are responsible for the generation of locomotor behavior in most animals. They are usually modeled in robotics as coupled dynamical systems that can reproduce periodic coordinated locomotion patterns [9], [10], [11]. From that point of view, rhythmic DMPs can be thought as an instance of a CPG.

Most contributions in CPGs and rhythmic DMPs are interested in the problem of learning a periodic motion [11], [7], [8] or generating coordinated periodic patterns with certain phase relationships and sensory feedback integration [11], [9]. However, the problem of generating the *transient* motion from an initial state to the periodic state is rarely addressed. There has been work on combining both discrete and rhythmic motions [12] but the shape of the transient motion cannot be controlled.

Nevertheless, all periodic motions must be started in a non-periodic way before the repeating pattern comes into play. Starting the motion cannot be a mere reproduction of part of the periodic pattern. For instance, when one is standing and then starts walking, the first step is different from the other following steps. Or when juggling, the balls have to be thrown up in the air at first before one can juggle the balls in a periodic motion. And all of these transient motions depend on the initial state of the robot (i.e. how are the feet on the ground when walking start or how are the balls distributed in the hands when juggling) and on the task to accomplish. There can therefore be several transients associated to one periodic task.

Because of these two observations (a) that there is a connection between the transient part and the periodic movement and (b) that there can be multiple independent transients, we want a system that is able to encapsulate the periodic pattern and its transients into a unit. This unit character should apply to both learning and executing the movement.

Addressing the problem of encoding the transient behavior will also help us address a conceptual issue that arises when we compare rhythmic and discrete DMPs. Discrete DMPs are dynamical systems with a stable fixed point (a 0 dimensional attractor) that encode the "way" to go to the attractor, i.e. the transient behavior from an initial start to the fixed point. From that point of view, rhythmic DMPs are conceptually different: although they also consist of a stable attractor (in this case a 1-D attractor: the limit cycle), the only thing that is encoded is the actual shape of this attractor. The transient behavior is never encoded.

In this contribution, we propose a formulation for rhythmic DMPs that includes both transient and periodic motion. It is possible to include several transient behaviors with the periodic motion into a single system. With this formulation, we

also make these motion primitives conceptually equivalent to their discrete counterpart since we can control the shape of both the transients and the attractor. We also demonstrate the capabilities of the theoretical construction with experiments on the ARMAR-III humanoid robot.

A. Overview of this approach

A DMP can be split into two parts: the *canonical system* and the *transformation system*. While the canonical system defines the state of the DMP in time, the transformation system is the link between this DMP state and the robot. The transformation system can be easily adapted to a desired trajectory, i.e. by solving a standard regression problem. The canonical system determines the type of attractor which can be either discrete or periodic.

Since we want to encode both, transient and periodic movement, we use a *two dimensional* canonical system. One dimension represents the current phase of the periodic motion while the other dimension corresponds to the distance of the current state towards the periodic pattern. Therefore, a canonical system with a unique limit cycle on the plane is used, c.f. Fig. 1(a). While the system advances towards the limit cycle it generates the desired transient. When the system has come close to the limit cycle, the generation of the periodic pattern starts.

By creating multiple paths towards the the limit cycle it is possible to encode multiple transients for the same periodic pattern. For this purpose, each of the paths encodes another transient behavior, see Fig. 1(c).

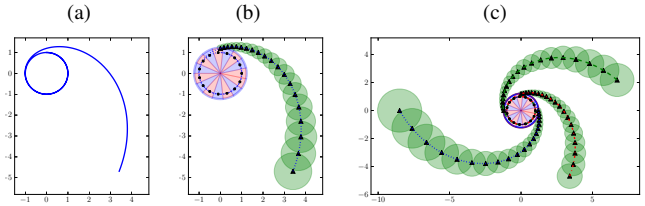

Fig. 1. Plot (a) shows a typical run of the canonical system ending up in the stable limit cycle. Considering (ϕ, r) as polar coordinates, this gives a circle around the origin, i.e. $(0, 0)$, with fixed radius, e.g. 1. In plot (b) the supports of the perturbation's basis functions are visualized. Each black dot on the limit circle represents a periodic basis function and the ring is the union of all supports of these. Each small triangles stands for a basis function encoding the transient part and the circles around them visualize the extend of their support. The right plot (c) shows the same for three different transients.

II. The new DMP formulation

In this section the concrete formulation for the DMP is presented.

A. The general idea of Dynamic Movement Primitives

As already stated, each DMP consists of two parts:

$$\begin{cases} \dot{s}(t) = \text{Canonical}(t, s), & (1) \\ \dot{y}(t) = \text{Transform}(t, y) + \text{Perturbation}(s). & (2) \end{cases}$$

The perturbation term in (2) is adapted to induce a desired behavior in the system, i.e. reproducing a given trajectory.

Furthermore, [13] and [7] demonstrated that the incorporation of appropriate feedback terms within a DMP allow the on-line adaption of the learned trajectory. In this way, movements can be generated under consideration of dynamical constraints such as obstacle avoidance or joint limit constraints.

B. Preliminaries and Terms

The process of learning a demonstrated motion be considered as the problem of function approximation. Hence, given a trajectory $y_{\text{demo}} : [0, \infty) \to \mathbb{R}$ (we use *function* and *trajectory* synonymously), we desire a system which provides $y : [0, \infty) \to \mathbb{R}$ being similar to the original trajectory. In our applications, the values of y_{demo} describe the evolution of one degree of freedom in time.

To shorten the notation in the following, some basic properties of functions are recalled.

Definition 1. *Let $D \subset \mathbb{R}$, A, B be sets and $f : D \to \mathbb{R}$, $g : A \to B$ be functions.*

1) *For $C \subset A$ the function $g|_C \to B$, $g|_C(x) := g(x)$ for all $x \in C$, is called* the restriction of g to C.
2) *If there is a $\tilde{p} > 0$ such that $f(x + \tilde{p}) = f(x)$ for all $x \in D$ then f is called* periodic. *In this case the number*

$$p := \inf \{p > 0 : f(x + p) = f(x) \text{ for all } x \in D\}$$

is called the period of f. *We also say that f is p-*periodic.
3) *Let $D = [0, \infty)$. If there exists a $\tilde{T} > 0$ such that the restriction $f|_{[\tilde{T}, \infty)}$ is periodic, we define*

$$T := \inf \left\{\tilde{T} > 0 : f|_{[\tilde{T}, \infty)} \text{ is periodic}\right\}$$

to be the transient length of f. *Further, in this case $f|_{[0,T)}$ is the* transient part of f. *We call $f|_{[T,\infty)}$* the periodic part of f *and say that f is* composed-periodic with period p, *where p is the period of $f|_{[T,\infty)}$. In the following we will write $\tilde{f} := f|_{[T,\infty)}$ for the periodic part of a composed-periodic trajectory f with transient length T.*

Simply spoken, the transient length T is the shortest time one has to wait until the trajectory becomes periodic.

From now on, let $y_{\text{demo}} : [0, \infty) \to \mathbb{R}$ be a composed-periodic trajectory with transient length $T > 0$ and period length $p > 0$. The restriction of having only one trajectory and hence only a single transient is used for simplicity reasons and will be lifted in Section V-A.

C. The Canonical System

The canonical system (see (1)) for the new DMP formulation is an oscillator in the phase plane. It is defined by $s(t) := (\phi(t), r(t))^T \in \mathbb{R} \times (0, \infty)$ for ϕ, r solving

$$(3) \quad \begin{cases} \dot{\phi} = \Omega, & (3a) \\ \dot{r} = \eta(\mu^\alpha - r^\alpha)r^\beta, & (3b) \\ \phi(0) = \phi_0, \ r(0) = r_0. & (3c) \end{cases}$$

Here, $\mu > 0$ denotes the radius of the limit cycle and $\eta, \alpha, \beta > 0$ are constants. The value of $\Omega > 0$ defines the angular velocity of ϕ and has to be chosen according to the period of the desired trajectory y_{demo}, i.e. $\Omega = \frac{2\pi}{p}$.

The values $\phi_0 \in \mathbb{R}$ and $r_0 > 0$ are initial conditions which have to be chosen individually for each desired transient. How to determine these values is explained in Section III-D. It can be shown that μ is a globally stable fixed point for r, i.e. for each $r_0 > 0$ it holds $r(t) \to \mu$ for $t \to \infty$.

The speed and shape of convergence of $r(t)$ to μ can be adjusted with α, β, and η. We used the values $\mu = 1$, $\eta = 35$, $\alpha = \frac{1}{6}$, and $\beta = \frac{1}{1000}$ which were determined experimentally.[1]

The solution is unique for each pair of initial conditions (ϕ_0, r_0). Therefore, two different approaches towards the limit cycle cannot intersect each other. This becomes important when more than one transient has to be encoded since it is desirable that different transient cannot affect each other.

Fig. 2 shows examples of solutions using (3) with different initial conditions.

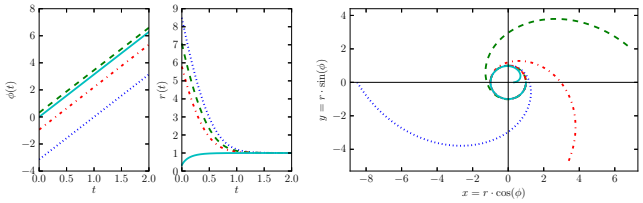

Fig. 2. Four simulation runs of the canonical system using different initial conditions. The convergence of the limit radius $\mu = 1$ is visible.

D. The Transformation System

The transformation system is a critically damped spring system with one global point attractor given by

$$\begin{cases} \dot{z} = \Omega\Big(\alpha_z\big(\beta_z(g - y) - z\big) + f(\phi, r)\Big), \\ \dot{y} = \Omega z. \end{cases} \tag{4}$$

This is a standard transformation system, see [7]. The constants $\alpha_z, \beta_z > 0$ are chosen according the ratio $\frac{\alpha_z}{\beta_z} = \frac{4}{1}$ in order to ensure critical damping. With $f \equiv 0$ the system state y converges to the anchor point $g \in \mathbb{R}$. By adapting f corresponding to the demonstrated trajectory y_{demo} the system oscillates around g in a similar manner as featured by y_{demo}. Here, f is defined as

$$f(\phi, r) = \frac{\sum_{j=1}^{M} \psi_j(\phi, r)\tilde{w}_j + \sum_{i=1}^{N} \varphi_i(\phi, r) w_i}{\sum_{j=1}^{M} \psi_j(\phi, r) + \sum_{i=1}^{N} \varphi_i(\phi, r)}, \tag{5}$$

where $W := (w_1, \ldots, w_N, \tilde{w}_1, \ldots, \tilde{w}_M)^T \in \mathbb{R}^{N+M}$ contains the weights which can be adjusted to fit the desired trajectory and

$$\psi_j : \mathbb{R} \times (0, \infty) \to \mathbb{R}, \quad j = 1, \ldots, M,$$
$$\varphi_i : \mathbb{R} \times (0, \infty) \to \mathbb{R}, \quad i = 1, \ldots, N$$

[1]The canonical system works for all $\eta, \alpha, \beta, \mu > 0$. The values we have chosen lead to a well shaped convergence allowing us to place the supports of the basis functions properly on the phase plane.

are the basis functions. While ψ_j are functions encoding the transient part of the motion, the functions φ_i are 2π-periodic in the first argument, and encode the periodic pattern. The vector of basis functions can be described as

$$\Psi := (\varphi_1, \ldots, \varphi_N, \psi_1, \ldots, \psi_M). \tag{6}$$

The crucial point in (4) and (5) is the perturbation force f which depends on *two* parameters, namely the state (ϕ, r) of the canonical oscillator. The first parameter ϕ denotes the phase of the motion whereas the second one r represents the distance from the limit cycle.

III. Connecting the Canonical System and the Transformation System

As pointed out in the previous section, ψ_j is used to encode the non-periodic transient behavior and φ_i to encode the periodic pattern. This means that in the beginning of the movement the system should be only affected by ψ_j while in the long run their impact vanishes and φ_i smoothly begin to take over the control of the system.

Considering the convergence behavior of the canonical system, c.f. the right plot in Fig. 2, the idea is to use the path to the limit cycle for encoding the transient part of y_{demo} and the limit cycle itself for the periodic pattern.

To explain the properties of the basis functions ψ_j and φ_i the following definition is useful.

Fix $n \in \{1, 2\}$ and a small[2] $\delta > 0$ and let $b : \mathbb{R}^n \to \mathbb{R}$ be a function. The set of $x \in \mathbb{R}^n$ where b does not vanish is called the *support of b (with respect to δ)*, i.e.

$$\mathbf{supp}_\delta\, b := \{x \in \mathbb{R}^n : |b(x)| \geq \delta\} \subset \mathbb{R}^n.$$

Fig. 1(b),(c) visualize the supports of the basis functions ψ_j and ϕ_i.

A. Fading from Transient to Periodic Movement

The basis functions ψ_j affect the transient part of the motion only and should not have an impact on the periodic pattern. Therefore, ψ_j vanish close to the limit cycle, i.e. there exists a $\mu_1 > \mu$ such that $\psi_j|_{\mathbb{R}\times(0,\mu_1)} = 0$. After passing the limit μ_1, the φ_i dominates the control of the system. Hence, the condition $\varphi_i|_{\mathbb{R}\times(0,\mu_1)} = 1$ holds. The value of μ_1 is a constant that can be chosen arbitrarily. In the course of experiments, we determined that $\mu_1 = 1.2\mu$ is a reasonable choice.

Since the movement should be smooth, there has to be a region where the supports of the φ_i and the ψ_j overlap. The time needed for the canonical oscillator to pass that region is called *transient fading time* t_f.

To create the fading region, $\mu_2 > \mu_1$ is set forcing the supports of φ_i and ψ_j at most overlap for $r \in (\mu_1, \mu_2)$. Here, μ_2 is chosen such that the transient fading time which the oscillator (3) needs to converge from μ_2 to μ_1 is equal to t_f. Fig. 3 visualizes the resulting overlapping of the basis function's supports and the radii μ_1, μ_2.

[2]Here, typically $\delta \approx 10^{-3}$.

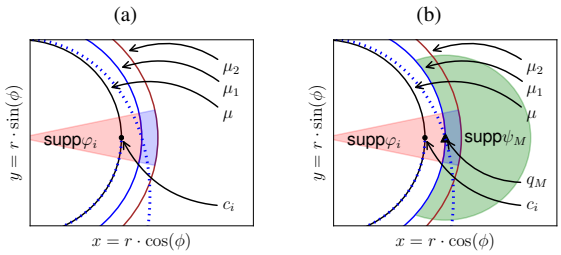

Fig. 3. Plot (a) shows the support of one periodic basis function φ_i located at the center c_i on the limit cycle with radius μ. In (b), the support of the last transient basis function ψ_M is added. The dotted line denotes the trajectory generated by the canonical system on the phase plane. Observe that the clipped circle results from the function a, c.f. (9), which is 0 for $r < \mu_1$.

B. Encoding the periodic movement

The basis functions φ_i encode the periodic pattern and thus should vanish away from the limit cycle. Therefore, φ_i is composed of two functions $g : (0, \infty) \to \mathbb{R}$ and $h_i : \mathbb{R} \to \mathbb{R}$ as follows

$$\varphi_i(\phi, r) = g(r)h_i(\phi).$$

Here, h_i is 2π-periodic and encodes the periodic pattern. The function g makes φ_i vanish away from the limit cycle, i.e.

$$g|_{(0,\mu_1)} = 1 \qquad \text{and} \qquad g|_{(\mu_2,\infty)} \approx 0. \tag{7}$$

For our experiments presented in the following we used

$$h_i(\phi) = \exp\Big(v_i\big(\cos(\phi - c_i) - 1\big)\Big),$$
$$g(r) = \begin{cases} 1, & r \in (0, \mu_1], \\ \exp\big(-\tilde{v}(r - \mu_1)^k\big), & r \in (\mu_1, \infty), \end{cases} \tag{8}$$

where $v_i > 0$ determines the width of $\mathbf{supp}_\delta\, h_i$, c.f. Fig. 4(b). Setting $c_i := (i-1)\frac{2\pi}{N}$ distributes the h_i uniformly over the limit cycle. The value $\tilde{v} > 0$ is chosen such that g satisfies (7). Note that g is k times continuously differentiable on $(0, \infty)$ for fixed $k \in \mathbb{N}$.[3] Fig. 4 provides example plots of φ_i, g and h_i.

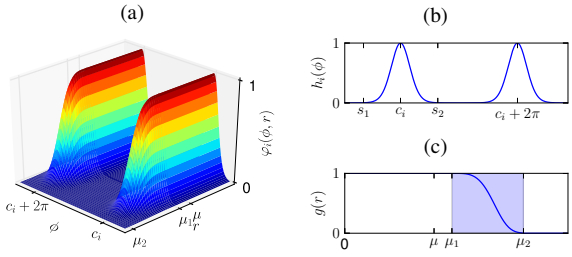

Fig. 4. Plot (a) shows two peaks of a periodic basis function φ_i centered at c_i. In (b) the projection onto the ϕ axis, i.e. h_i, is shown. The values s_1 and s_2 mark the borders of $\mathbf{supp}_\delta\, h_i$. Plot (c) shows the projection onto the r axis, i.e. g. Here, the interval $[\mu_1, \mu_2]$ used for fading is highlighted.

Using polar coordinates $\mathbf{supp}_\delta\, \varphi_i$ is projected onto the phase plane leading to a circular sector with radius μ_2 where the angle depends on v_i. The value of c_i rotates the projection of the support around the origin, c.f. Fig. 3.

[3]We used $k = 4$ which makes the perturbation force smooth and leads to the desired fading behavior.

C. Encoding the transient movement

The basis functions ψ_j are arranged on the phase plane away from the limit cycle as shown in Fig. 1, where the small triangles symbolize the centers of the functions ψ_j and the circles visualize the extend of their support. Similarly to the φ_i, the ψ_j are composed of two functions: one for the actual encoding and another one for keeping them away from the limit cycle. Hence, each function ψ_j has the form[4]

$$\psi_j(\phi, r) = a(r)b_j\big(\|\mathbf{pol}(\phi, r) - q_j\|_2\big)$$

where the function $a : (0, \infty) \to \mathbb{R}$ ensures that the ψ_j are nonzero only away from the limit cycle. The function $b_j : \mathbb{R} \to \mathbb{R}$ is a standard basis function which can be represented in the form of a Gaussian, see e.g. [1]. Placing the norm difference into b_j leads to a radially symmetric function centered around $q_i \in \mathbb{R}^2$ on the phase plane. Here, we used

$$a(r) = \begin{cases} \exp\big(-\tilde{v}(r - \mu_2)^k\big), & r \in (0, \mu_2), \\ 1, & r \in [\mu_2, \infty), \end{cases} \tag{9}$$
$$b_j(r) = \exp\big(-\bar{v}r^2\big).$$

The function a is an analogon to the g in the definition of φ_i, c.f. (8). By choosing the $\tilde{v}$ as in (8) the function a satisfies a condition symmetric to (7) with the same μ_1, μ_2, c.f. Fig. 4(c) and Fig. 5(c).

For each ψ_j, we choose a $\delta_j > 0$ defining the radius of the support for the ψ_j. Fig. 5 depicts an exemplary plot. The centers q_i and radii δ_j are chosen in such a way, that

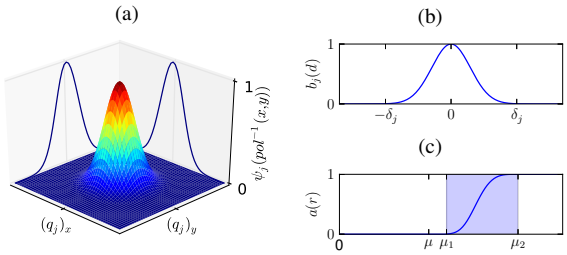

Fig. 5. In (a) a basis function ψ_j with center q_j is shown. Plot (b) shows the distance function b_j, where δ_j determines the support's radius. The function a, used make $\psi_j(\phi, r) = 0$ for $r < \mu_1$, is shown in (c). As in Fig. 4 the fading interval $[\mu_1, \mu_2]$ is highlighted.

basis functions ψ_j are uniformly distributed in time, i.e. the duration of influence is identical for each basis function. By doing so the same approximation resolution is attained everywhere assuming that we have no a priori knowledge about the demonstrated trajectory y_{demo}.[5]

Fig. 6 visualizes the fading interval and shows the resulting influence of the basis functions over time.

[4]Here, $\mathbf{pol}(\phi, r) = \big(r\cos(\phi), r\sin(\phi)\big)$ is the polar coordinate mapping and $\|x\|_2$ denotes the Euclidean norm of $x \in \mathbb{R}^2$.

[5]Choosing the support of the ψ_j according to the changing behavior of y_{demo} is a possible extension which is not discussed in this work.

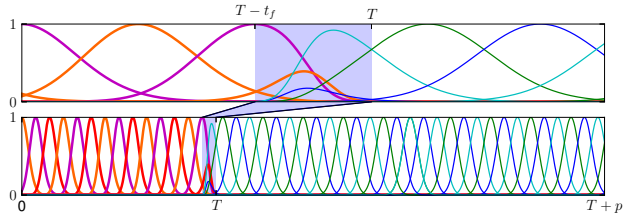

Fig. 6. The plot shows the graphs of all basis functions ψ_j and φ_i over time, i.e. the graphs of all functions $\hat{b}(t) = b\big(\phi(t), r(t)\big)$ for each component $\hat{b}$ of Ψ, cf. (6). Here, $\big(\phi(t), r(t)\big)$ is the solution of the canonical system (3) at time t. Therefore, each peak corresponds to a basis function ψ_j or φ_i respectively. The plot shows $M = 15$, $N = 30$ basis functions for a transient length T and a period duration of $p = 2T$. Note that for $t < T - t_f$ the transient basis functions ψ_j drive the system whereas the φ_i gain complete control after $t = T$.

D. Selecting initial conditions of the canonical system for a given transient length

In order to parameterize the canonical system with respect to the desired trajectory, a mapping $\mathbf{init}_T$ is to be defined which yields the initial values ϕ_0, r_0 such that the canonical oscillator reaches a desired state $(\tilde{\phi}, \tilde{r})$ after the transient length T.

Given a fixed pair $(\tilde{\phi}, \tilde{r}) \in \mathbb{R} \times (0, \infty)$, exactly one pair of initial conditions $(\phi_0, r_0) \in [0, 2\pi) \times (0, \infty)$ exists for the canonical system (3) such that the oscillator reaches $(\tilde{\phi}, \tilde{r})$ after the transient length T of y_{demo}, i.e.[6]

$$r(t) \begin{cases} > \tilde{r}, & t < T, \\ = \tilde{r}, & t = T, \\ < \tilde{r}, & t > T, \end{cases} \qquad \phi(t) \begin{cases} < \tilde{\phi}, & t < T, \\ = \tilde{\phi}, & t = T, \\ > \tilde{\phi}, & t > T. \end{cases}$$

Therefore, we can define the mapping $\mathbf{init}_T$ by

$$\mathbf{init}_T(\tilde{\phi}, \tilde{r}) := (\phi_0, r_0).$$

E. Learning a given trajectory

To adapt the system to a given trajectory y_{demo}, the canonical system (3) has to be initialized such that the DMP generates a composed-periodic trajectory with transient length T. Therefore, we choose

$$(\phi_0, r_0) := \mathbf{init}_T(0, \mu_1),$$

in order to enforce the system to reach the radius μ_1 after time T while for the phase $\phi(T) = 0$ holds.[7]

Further, the weights $W \in \mathbb{R}^{N+M}$ in (5) have to be adjusted to fit the demonstrated trajectory y_{demo}. This is done by rearranging (4) to the perturbation f and replacing $z = \frac{\dot{y}}{\Omega}$, $\dot{z} = \frac{\ddot{y}}{\Omega}$. For each time $t \in [0, \infty)$ one obtains

$$f\big(\phi(t), r(t)\big) = \frac{\ddot{y}(t)}{\Omega^2} - \alpha_z \left(\beta_z \big(g - y(t)\big) - \frac{\dot{y}(t)}{\Omega} \right). \quad (10)$$

Inserting y_{demo}, $\dot{y}_{\text{demo}}$, $\ddot{y}_{\text{demo}}$ into (10) results in a perturbation force value $f_{\text{targ}}\big(\phi(t), r(t)\big)$ for each pair $\big(\phi(t), r(t)\big)$.

[6]The assertions for ϕ are meant modulo 2π.

[7]Here, the entrance phase $\phi(T)$ can be chosen arbitrarily. The entrance phase becomes important when more than one transient is encoded, see Section V.

In practice, only $L \in \mathbb{N}$ discrete samples of the trajectory y_{demo} are known, i.e. $y_{\text{demo}} = \big(y_{\text{demo}}(t_1), \dots, y_{\text{demo}}(t_L)\big)$. Hence, $(\phi_l, r_l) := \big(\phi(t_l), r(t_l)\big)$ and the corresponding $f_{\text{targ}}(\phi_l, r_l)$ for $l = 1, \dots, L$ are calculated using (10). Fitting these values to the perturbation representation in (5) leads to a locally linear weighted regression problem for the weight vector W, i.e.

$$W_i := \arg\min_{w \in \mathbb{R}} \sum_{l=1}^{L} \Psi_i(\phi_l, r_l) \big(f_{\text{targ}}(\phi_l, r_l) - w\big)^2, \quad (11)$$

for $i = 1, \dots, M+N$. This problem can be solved efficiently by standard linear regression methods, see e.g. [14].

Note that *all* weights, those related to the transient and those related to the periodic pattern, can be calculated all at once by solving (11).

IV. Experiments

The proposed DMP formulation has been implemented on the humanoid robot ARMAR-IIIb to enable the learning of periodic actions such as wiping through human observation. For this purpose, motion data of human wiping demonstrations were recorded using a marker-based human motion capture system provided by Vicon [15]. With markers placed on the hand and the wrist of the human subject trajectories describing hand's wiping movements in task-space were captured at a frequency of 100 Hz. In our experiments, four styles of wiping movements were investigated which feature varying discrete initial approach movements (simple and complex) and different periodic wiping patterns (circle and figure eight), see Fig. 7. The captured human demonstrations and the generated trajectories using the correlating DMP are illustrated in Fig. 7. Experiments with multiple approach movements as described in Section V have not been conducted yet.

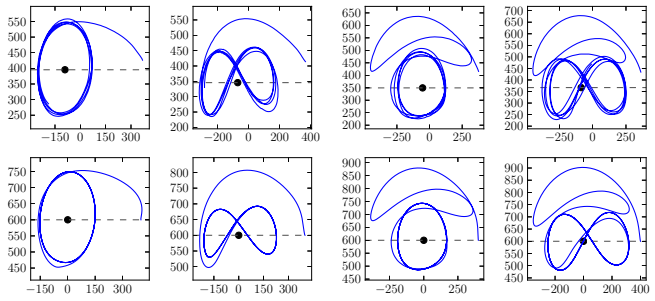

Fig. 7. From the left to right plot all recorded wiping styles (1,2,3,4) are shown. The top line shows the original motion that was captured from human demonstration. On the bottom, the corresponding trajectories generated by the DMP are visualized. Note the different starting and anchor points indicated by the dashed lines.

In order to apply the proposed DMP formulation to a recorded trajectory $y_{\text{demo}} = (y_1, \dots, y_L)$ with corresponding times $t_1, \dots, t_L$ we need to determine the transient fading time t_f, the period p and the anchor point g.

For that reason, we segmented the trajectory into two parts, i.e. $y_{\text{trans}} = (y_1, \dots, y_{L_{\text{trans}}})$ and $y_{\text{per}} = (y_{L_{\text{trans}}+1}, \dots, y_L)$.

The segment y_{trans} contains the data points corresponding to the transient part and y_{per} is the vector of data points corresponding to the periodic pattern.

By this segmentation we obtain the transient fading time as the duration of the transient part, i.e. $t_f = t_{L_{\text{trans}}+1}$, and the anchor point as the mean of all points of the periodic part, i.e.

$$g = \frac{1}{L - L_{\text{trans}}} \sum_{k=L_{\text{trans}}+1}^{L} y_k.$$

The segmentation itself was done algorithmically.

We employed $M = N = 40$ basis functions to represent the demonstrated movements. Fig. 8 shows the convergence behavior for an increasing number of basis functions to approximate a synthesized function.

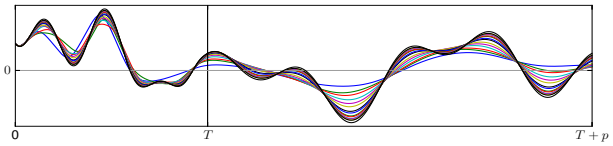

Fig. 8. The plot shows the convergence behavior for an increasing number of basis functions to a synthesized signal. The thick plot corresponds to the original trajectory which is approximated by the presented DMP using different counts of basis functions. Concretely, $N = M = 10, 14, 20, 27, 35, 40$ basis functions have been used.

In order to synthesize the learned wiping movement on the robot, the DMP is parameterized with scene-specific start and anchor position.

The capability of this DMP formulation regarding the generalization to different start and anchor positions is shown in Fig. 9.

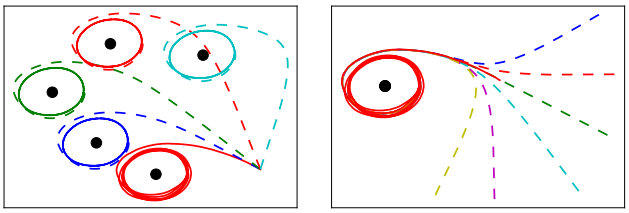

Fig. 9. On the left the generalization to different anchor points (black dots) is visualized. The right plot shows runs with different starting points of the same motion. All dashed plots show reproductions of wiping style 1 and the solid line corresponds to the original trajectory.

In our experiments, for each DMP wiping movements were generated starting from three points and leading to three different goal positions which are equivalent to the anchor points of the periodic pattern.

By integrating the resulting control policy and using differential kinematics the wiping movements could be reproduced on our experimental platform the humanoid robot ARMAR-IIIb (see Fig. 10). ARMAR-IIIb is a copy of the robot ARMAR-IIIa (see [16]) and consists of seven subsystems: head, left arm, right arm, left hand, right hand, torso, and a mobile platform in the form of a wheel-based holonomic

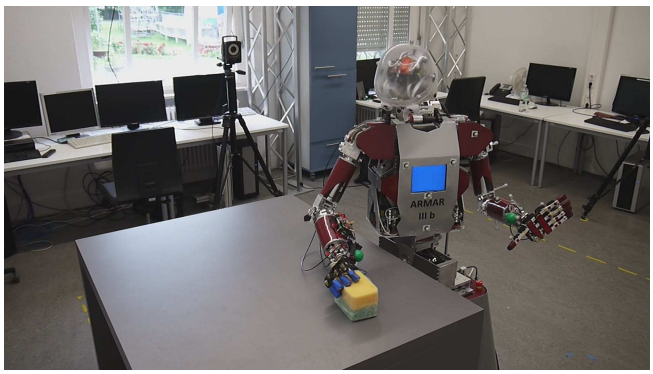

Fig. 10. The humanoid platform ARMAR-IIIb wiping the table with a sponge using the presented DMP formulation.

platform. The upper body of the robot provides 33 DoF: $2 \cdot 7$ DoF for the arms and three DoF for the torso. The arms are designed in an anthropomorphic way: three DoF for each shoulder, two DoF in each elbow and two DoF in each wrist. Each arm is equipped with a five-fingered hand with eight DoF. A force torque sensor between the wrist and the hand of the robot allows measurements of external forces exerted on the robot's TCP.

Due to inaccuracies within the kinematic chain from platform to the robot's TCP, contact with the surface to be wiped and the wiping tool cannot be guaranteed. To attain a goal-directed reproduction of the learned wiping action, we exploit the force torque sensor in order to adapt the vertical movement of the TCP to the surface shape during the execution of the generated wiping movement. This additional online force adaptation step requires a further reduction of the reproduction speed. Hence, the wiping movements could be reproduced at half of the demonstrated speed. In order to visualize the executed robot trajectories, a pen is attached to the sponge. To minimize the friction between the sponge and the surface, only soft pressure is applied during the wiping. Hence, contact is already determined if only parts of the sponge, not necessarily the pen, touch the surface leading to discontinuities in the drawn trajectories. The results of the experiments are depicted in Fig. 11 and can be reviewed in the attached video.

V. Generalization

In this section we will outline how to generalize the DMP to handle multiple transients and multiple output dimensions.

A. Encoding and learning multiple transients

In order to to encode multiple transient parts, we assume that, instead of a single trajectory, a set of composed-periodic trajectories $y^1_{\text{demo}}, \ldots, y^K_{\text{demo}} : [0, \infty) \to \mathbb{R}$, $K \in \mathbb{N}$, with common periodic part is given.[8] The corresponding transient lengths are denoted by $T_1, \ldots, T_K$.

Different trajectories can enter the common periodic part at different phases. Therefore, we will define the *phase shift*

[8]Throughout this section, the exponents are indices.

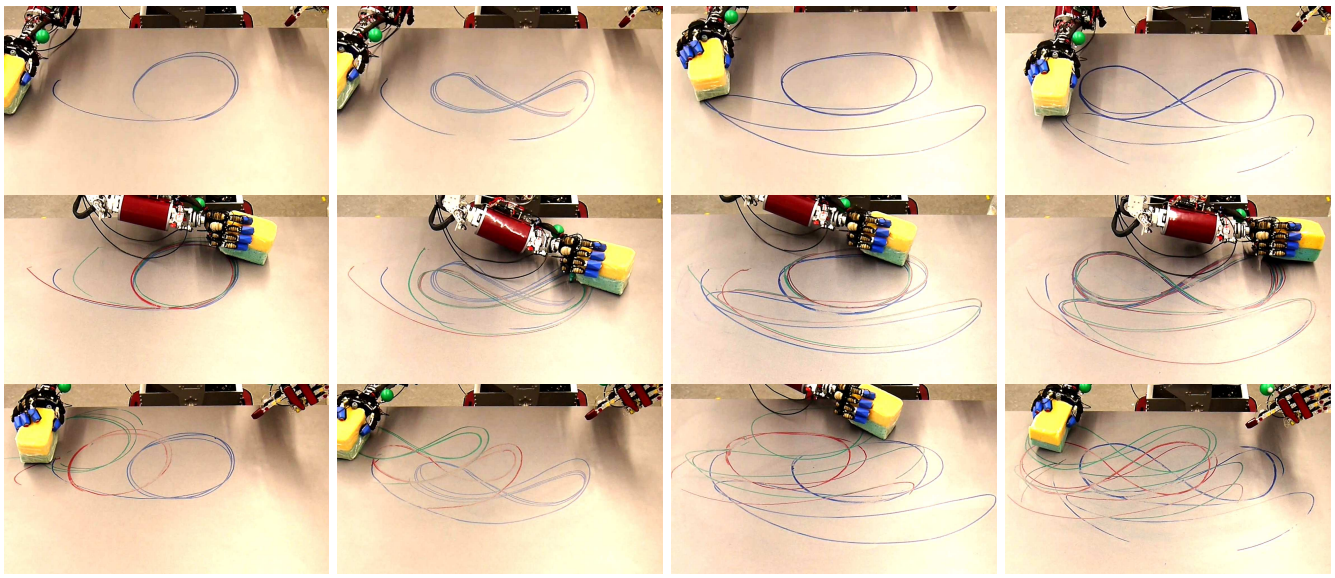

Fig. 11. Top: Single reproduction of a wiping movement from style 1, 2, 3, and 4. The trajectory is drawn using a pen attached to the sponge. Middle: Multiple reproductions of a wiping movement with different start positions. Bottom: Multiple reproductions of a wiping movement with different goal positions (equivalent to the anchor points of the periodic pattern).

that determines how far the trajectories have to be shifted relatively to each other to align the periodic pattern.

Considering two p-periodic functions $a, b : \mathbb{R} \to \mathbb{R}$, if there is a $s > 0$ with $a(t) = b(t + s)$ for all $t \in \mathbb{R}$ we call a and b to be *shifted in phase* and define the *phase shift of a and b* by

$$\mathbf{ps}\,(a, b) := \min\{s \geq 0 : a(t) = b(t + s) \text{ for all } t \in \mathbb{R}\}.$$

It is assumed that the periodic parts $\tilde{y}^1_{\text{demo}}, \ldots, \tilde{y}^K_{\text{demo}}$ are pairwisely shifted in phase.[9] Since we want to encode all trajectories with the a single canonical system, a common phase ϕ is needed. To achieve this, we select the trajectory with the shortest transient length, say $y^{k_0}_{\text{demo}}$, and shift all the other trajectories such that the periodic pattern are in-phase. Hence, it is defined that the trajectory with the shortest transient length enters the periodic pattern at $\phi = \hat{\phi}^{k_0} := 0$. The other trajectories are aligned relatively to $y^{k_0}_{\text{demo}}$ according to the corresponding phase shifts $s_k := \mathbf{ps}\left(\tilde{y}^{k_0}_{\text{demo}}, \tilde{y}^k_{\text{demo}}\right)$. This leads to entrance phases $\hat{\phi}^k = \frac{2\pi}{p} s_k$, $k = 1, \ldots, K$, of the canonical system. For each trajectory y_{demo} we obtain initial conditions $(\phi^k_0, r^k_0) \in [0, 2\pi) \times (0, \infty)$ of the canonical oscillator by

$$(\phi^k_0, r^k_0) := \mathbf{init}_{T_k}\left(\hat{\phi}^k, \mu_1\right), \qquad k = 1, \ldots, K.$$

Each transient has its own set of $M_k \in \mathbb{N}$ basis functions $\psi^k_1, \ldots, \psi^k_{M_k} : \mathbb{R} \times (0, \infty) \to \mathbb{R}$ and therefore the perturbation term in (5) gets extended to

$$f(\phi, r) = \frac{\sum_{k=1}^{K} \sum_{j=1}^{M_k} \psi^k_j(\phi, r)\tilde{w}^k_j + \sum_{i=1}^{N} \varphi_i(\phi, r) w_i}{\sum_{k=1}^{K} \sum_{j=1}^{M_k} \psi^k_j(\phi, r) + \sum_{i=1}^{i} \varphi_i(\phi, r)}.$$

[9]Here $\tilde{y}_{\text{demo}}$ is the periodic part of y_{demo}, see Definition 1.

Further, we set $D := \sum_{k=1}^{K} M_k + N$ to be the total number of basis functions and extend the vector of weights and the vector of basis function to

$$W := (w_1, \ldots, w_N, \tilde{w}^1_1, \ldots, \tilde{w}^1_{M_1}, \ldots, \tilde{w}^k_1, \ldots, \tilde{w}^k_{M_k})^T,$$
$$\Psi := (\varphi_1, \ldots, \varphi_N, \psi^1_1, \ldots, \psi^1_{M_1}, \ldots, \psi^k_1, \ldots, \psi^k_{M_k}).$$

Note that both, W and Ψ, consist of D components.

In practice, we know just samples of the demonstrated trajectories, i.e. each y^k_{demo} consists of $L_k \in \mathbb{N}$ discrete data points. Therefore, we have $y^k_{\text{demo}} = (y^k_1, \ldots, y^k_{L_k})$ where $y^k_l = y^k_{\text{demo}}(t^k_l)$, $l = 1, \ldots, L_k$, are the values at the given discrete time samples t^k_l. We obtain the corresponding states of the canonical system by $(\phi^k_l, r^k_l) := \left(\phi^k(t^k_l), r^k(t^k_l)\right)$. Here, the tuple of functions (ϕ^k, r^k) is the solution of the canonical system (3) for the initial conditions (ϕ^k_0, r^k_0). By inserting each demonstrated trajectory y^k_{demo} and the associated states of the canonical system (ϕ^k_l, r^k_l) into (10) the target perturbation force samples $f(\phi^k_l, r^k_l)$ are obtained for $l = 1, \ldots, L_k$.

Learning the trajectories is then achieved by solving the linear regression problem (12) for each $i = 1, \ldots, D$.

$$W_i := \arg\min_{w \in \mathbb{R}} \sum_{k=1}^{K} \sum_{l=1}^{L_k} \Psi_i(\phi^k_l, r^k_l)\left(f(\phi^k_l, r^k_l) - w\right)^2 \quad (12)$$

B. Driving more than one joint or more than one task space dimension

In order to encode the movement of multiple joints or a motion in multidimensional space we need to to approximate a multidimensional input trajectory $y_{\text{demo}} : [0, \infty) \to \mathbb{R}^D$, $y_{\text{demo}}(t) = \left(y_1(t), \ldots, y_D(t)\right)^T \in \mathbb{R}^D$. This can be achieved by assigning a separate transformation system T_j, c.f. (4), to each of the one-dimensional trajectories y_j. Then a

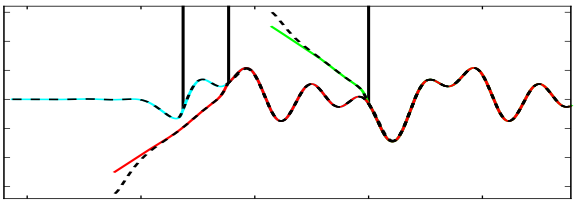

Fig. 12. The plot shows a synthetic signal over time featuring three different transients encoded using the generalization described in Section V-A. The vertical lines mark the entrance phase for each transient. By the dashed lines the reproductions from different initial conditions are visualized. Note that simple linear transients have been chosen in order to maintain clarity of the plot.

single canonical system C, see (3), is shared among these transformation systems. The DMP for the multidimensional demo trajectory is represented by the tuple $(C, T_1, \ldots, T_D)$. Sharing the canonical system synchronizes the outputs of the transformation systems. Note that each transformation system T_j features a distinct weight vector $W(j)$ obtained by solving (11) or (12) respectively for each dimension separately.

VI. Conclusion

In this work, we presented a DMP formulation which unifies the representation of a periodic movement and its transients. In order to do so, based on the DMP formulation presented in [7] we extended the canonical system by one dimension using a two dimensional oscillator. Further, we designed suitable basis functions. This formulation has been evaluated for the scenario of wiping. Based on human demonstrations of different wiping styles (featuring a discrete approach and the periodic movement) DMPs were learned and reproduced on a humanoid robot.

In order to attain a more general representation, in this work we presented a method which enables the encoding of multiple transients for the same periodic pattern. We provided a proof of concept evaluation using a synthetic pattern. Our experiments revealed limitations of the generalization properties of the used transformation system. For instance, scaled or rotated reproductions of the encoded movement are not possible with the presented formulation. Hence, we will examine the combination of alternative transformation systems with the new DMP. In this context, we will investigate how feedback can be incorporated to allow on-line adaption. For example, force profile learning similar to the approaches presented in [17], [5] and obstacle avoidance are of interest. In addition, we will investigate how to encode the end of the movement in a similar way as the transients.

Acknowledgment

This research was partially conducted within the International Center for Advanced Communication Technologies (interACT), was funded from the European Union Sixths and Seventh Framework Programme under grant agreement no. 270273 (Xperience), and supported additionally by National Science Foundation grants ECS-0326095, IIS-0535282, IIS-1017134, CNS-0619937, IIS-0917318, CBET-0922784, EECS-0926052, CNS-0960061, the DARPA program on Autonomous Robotic Manipulation, the Army Research Office, the Okawa Foundation, the ATR Computational Neuroscience Laboratories, and the Max-Planck-Society.

References

[1] A. J. Ijspeert, J. Nakanishi, and S. Schaal, "Movement imitation with nonlinear dynamical systems in humanoid robots," in *In IEEE International Conference on Robotics and Automation (ICRA)*, 2002, pp. 1398–1403.

[2] J. N. Auke Jan Ijspeert and S. Schaal, "Learning rhythmic movements by demonstration using nonlinear oscillators," in *In Proceedings of the IEEE/RSJ Int. Conference on Intelligent Robots and Systems (IROS)*, 2002, pp. 958–963.

[3] E. Theodorou, J. Buchli, and S. Schaal, "A generalized path integral control approach to reinforcement learning," *journal of machine learning research*, vol. 11, pp. 3137–3181, 2010. [Online]. Available: http://www-clmc.usc.edu/publications//T/theodorou10aNew.pdf

[4] H. Hoffmann, P. Pastor, D.-H. Park, and S. Schaal, "Biologically-inspired dynamical systems for movement generation: automatic real-time goal adaptation and obstacle avoidance," in *International Conference on Robotics and Automation (ICRA)*, 2009. [Online]. Available: http://www-clmc.usc.edu/publications/H/hoffmann-ICRA2009.pdf

[5] P. Pastor, L. Righetti, M. Kalakrishnan, and S. Schaal, "Online movement adaptation based on previous sensor experiences," in *IEEE/RSJ International Conference on Intelligent Robots and Systems (IROS)*, 2011. [Online]. Available: http://www-clmc.usc.edu/publications/P/pastor-IROS2011

[6] J. Nakanishi, J. Morimoto, G. Endo, G. Cheng, S. Schaal, and M. Kawato, "Learning from demonstration and adaptation of locomotion with dynamical movement primitives," *Robotics and Autonomous Systems*, vol. 47, pp. 79–91, 2003.

[7] A. Gams, A. J. Ijspeert, S. Schaal, and J. Lenarčič, "On-line learning and modulation of periodic movements with nonlinear dynamical systems," *Autonomous Robots*, vol. 27, no. 1, pp. 3–23, 2009.

[8] T. Petric, A. Gams, A. Ijspeert, and L. Žlajpah, "On-line frequency adaptation and movement imitation for rhythmic robotic tasks," *The International Journal of Robotics Research*, vol. 30, no. 14, pp. 1775–1788, Dec. 2011.

[9] H. Kimura, Y. Fukuoka, and A. Cohen, "Adaptive dynamic walking of a quadruped robot on natural ground based on biological concepts," *International Journal of Robotics Research*, vol. 26, no. 5, pp. 475–490, 2007.

[10] A. Ijspeert, "Central pattern generators for locomotion control in animals and robots: a review," *Neural Networks*, vol. 21, no. 4, pp. 642–653, 2008.

[11] L. Righetti and A. Ijspeert, "Programmable central pattern generators: an application to biped locomotion control," in *Proceedings of the IEEE International Conference on Robotics and Automation, ICRA*, 2006, pp. 1585–1590.

[12] S. Degallier, L. Righetti, S. Gay, and A. Ijspeert, "Toward simple control for complex, autonomous robotic applications: combining discrete and rhythmic motor primitives," *Autonomous Robots*, 2011.

[13] P. P. Dae-Hyung Park, Heiko Hoffmann and S. Schaal, "Movement reproduction and obstacle avoidance with dynamic movement primitives and potential fields," in *IEEE International Conference on Humanoid Robots, 2008.*, 2008.

[14] S. Schaal and C. G. Atkeson, "Constructive incremental learning from only local information," no. 8, pp. 2047–2084, 1998. [Online]. Available: http://www-clmc.usc.edu/publications/S/schaal-NC1998.pdf; http://www-clmc.usc.edu/publications/S/schaal-TRH209.pdf

[15] "Vicon Peak," Website, available online at http://www.vicon.com.

[16] T. Asfour, K. Regenstein, P. Azad, J. Schröder, N. Vahrenkamp, and R. Dillmann, "ARMAR-III: An integrated humanoid platform for sensory-motor control," in *IEEE/RAS International Conference on Humanoid Robots*, 2006.

[17] A. Gams, M. Do, A. Ude, T. Asfour, and R. Dillmann, "On-Line periodic movement and force-profile learning for adaptation to new surfaces," Nashville, USA, December 2010.